Excited-State Interactions in Pyrrolidinofullerenes

K. George Thomas,* V. Biju, and M. V. George*,†

Photochemistry Research Unit, Regional Research Laboratory, Trivandrum 695 019, India

Dirk M. Guldi*,‡ and Prashant V. Kamat*,§

Radiation Laboratory, University of Notre Dame, Notre Dame, Indiana 46556

Received: August 25, 1997; In Final Form: December 2, 1997

Two new pyrrolidinofullerenes, **1** and **2,** have been synthesized, and their photophysical properties have been investigated. The pyrrolidinofullerene **1** has three phenyl groups attached to the 1, 2, and 5 positions of the pyrrolidine ring. The pyrrolidinofullerene **2**, on the other hand, has a flexible attachment with an *N*-methylaniline end group and is the prototype of a fullerene−aniline dyad. Singlet and triplet excited-state properties of these two functionalized fullerene derivatives have been examined with picosecond and nanosecond laser flash photolysis. The singlet and triplet excited states of these fullerenes exhibit characteristic absorption bands in the vis-IR region of the spectrum. The functionalization of C_{60} with pyrrolidine groups shift the excited-state absorption maxima to the blue. Three different quenchers, O_2, TEMPO, and ferrocene, are employed to investigate the reactivity of triplet excited states. The bimolecular quenching rate constants determined for these quenchers were in the range of 5.3×10^8 to 7.7×10^9 M^{-1} s^{-1}. The excited-state interactions of these functionalized fullerenes are compared to that of C_{60}.

Introduction

Design of covalently linked donor−acceptor systems, which can mimic photosynthetic reaction center and generate long-lived radical pairs, employing photoinduced electron-transfer reactions are of considerable interest (see for example, ref 1−3). The efficiency of charge separation and recombination in such systems can be conveniently tuned by varying the redox properties of the donor as well as the acceptor and also the distance between them. The remarkable photophysical properties of fullerenes,[4−8] particularly their ability to undergo multistep[9−11] reduction, make them ideal acceptors for designing such molecular dyads.

Fullerenes form charge-transfer complexes with electron donors such as aromatic amines[12−15] but undergo nucleophilic addition reactions with aliphatic amines.[4,16,17] The free energy change, calculated for electron transfer from *N*,*N*-dimethylaniline to $^1C_{60}$ and $^3C_{60}$, indicates that this is an energetically favorable process ($\Delta G = -18.2$ and -9.8 kcal mol^{-1}, respectively).[4] The intermolecular photoinduced electron transfer in this system has been investigated by various groups [13−15,18,19] using transient absorption studies. More recently, Williams et al.[20,21] have studied the intramolecular electron-transfer processes in C_{60}-aniline dyads possessing rigid spacers. Preliminary results on the photophysical and electrochemical studies of a few *N*-phenylpyrrolidinofullerenes, prepared through the 1,3-dipolar cycloaddition of azomethine ylides to C_{60}, have been communicated in a recent communication.[22] Similar pyrrolidine derivatives of C_{60} have been used to modify SnO_2 electrodes for the purpose of developing photoelectrochemically active electrode materials.[23] Photoinduced electron-transfer processes in C_{60}-based dyads containing donors such as ferrocene,[24] porphyrin,[25,26] and carotenoid,[27] etc. have also been reported in the literature. In this paper, we report the synthesis and the detailed investigation on the photoinduced electron transfer of a novel C_{60} derivative **2** (Chart 1), covalently linked to aniline through a semiflexible chain. These results are compared with the excited-state properties of a similar compound, **1**, which has three phenyl substituents on the pyrrolidine ring. The intermolecular electron-transfer studies between **1** and *N*,*N*-dimethylaniline (DMA) are also presented.

CHART 1

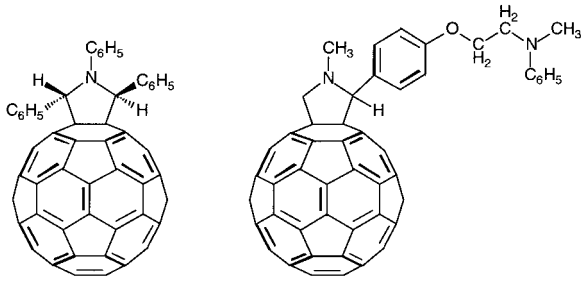

1 **2**

Experimental Section

Methods. All melting points are uncorrected and were determined on a Aldrich melting point apparatus. IR spectra were recorded on a Perkin-Elmer model 882 IR spectrometer and the UV−visible spectra on a Shimadzu 2100 or GBC 918 spectrophotometer. ^1H NMR and ^{13}C NMR spectra were recorded on either a JEOL EX-90 or Varian VXR 500S spectrometer. Mass spectra were recorded on a JEOL JMS AX 505HA mass spectrometer. The emission spectra were recorded

† Also at the Radiation Laboratory, University of Notre Dame, and the Jawaharlal Nehru Centre for Advanced Scientific Research, Bangalore 560 064, India (E-mail: mvg@csrrltrd.ren.nic.in).

‡ E-mail: Guldi@macroni.rad.nd.edu.

§ E-mail: KAMAT.1@ND.EDU or http://www.nd.edu/∼pkamat.

S1089-5639(97)02756-4 CCC: $15.00
Published on Web 01/30/1998

SCHEME 1

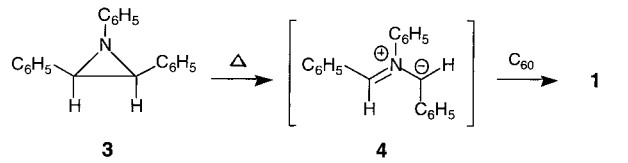

SCHEME 2

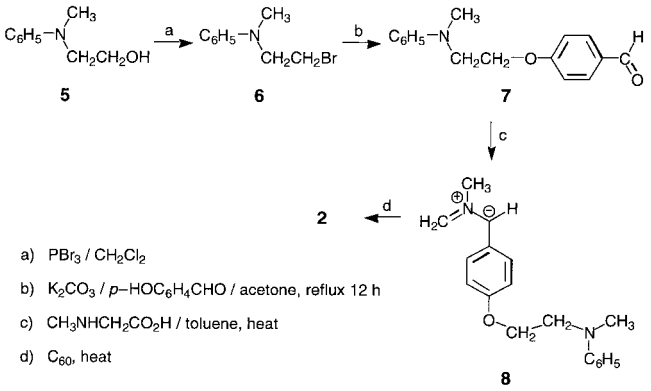

on SLM-8100 and Spex-Fluorolog, F112-X spectrofluorometers equipped with a 450 W Xe lamp and a Hamamatsu R928 photomultiplier tube. The excitation and emission slits were 4 and 1, respectively. A 570-nm long-pass filter was placed before the emission monochromator in order to eliminate the interference from the solvent, and no corrections were applied for the fluorescence spectra. Quantum yields of fluorescence were measured by a relative method using optically dilute solutions (absorbance was adjusted to 0.1 at 470 nm, and the emission intensity was measured at 713 nm). C_{60} dissolved in toluene ($\phi_f = 2.2 \times 10^{-4}$) was used as reference.[28] Spectroscopy-grade solvents were used for all measurements, and the solutions were purged with argon before use.

Starting Materials. The fullero-1,2,5-triphenylpyrrolidine **1** was synthesized through the 1,3-dipolar cycloaddition of the azomethine ylide **4** with C_{60} as shown in Scheme 1. The azomethine ylide **4** itself was generated through the thermal ring opening of 1,2,3-triphenylaziridine **3**. The starting triphenylazirdine **3**,[29] mp 99 °C, was prepared by a reported procedure. C_{60} was purchased from SES Corporation. Synthesis of the fullerene−aniline dyad **2** was achieved through the sequence of reactions shown in Scheme 2.

Synthesis of Fullero-1,2,5-triphenylpyrrylodine (1). A mixture of C_{60} (72 mg, 0.1 mmol) and **3** (27 mg, 0.1 mmol) in toluene (40 mL) was refluxed for 6 h. The reaction mixture was cooled, and removal of the solvent under reduced pressure gave a solid residue, which was chromatographed over silica gel. Elution with petroleum ether gave 20 mg (28%) of the unchanged C_{60}. Further elution with a mixture (1:4) of toluene and petroleum ether gave 30 mg (42%) of the monoadduct **1**, mp > ,400 °C. IR ν_{max} (KBr) 1601, 1500, 1543, 1450, 1265, 696 cm^{-1}; UV λ_{max} ($CHCl_3$) 257 nm (ϵ 123 000), 312 (38 000); ^1H NMR ($CDCl_3$) δ 6.68−6.82, 7.1−7.4, and 7.72−7.84 (17 H, m, methine and aromatic). Anal. Calcd for $C_{80}H_{17}N$: C, 96.94; H, 1.73; N, 1.41. Found: C, 96.63; H, 1.73; N, 1.21. Mol wt calcd for $C_{80}H_{18}N$ (MH^+) 992.1439; found, 992.1460 (FAB, high-resolution mass spectrometry).

Further elution of the silica gel column with a mixture (3:7) of toluene and petroleum ether gave 20 mg (28%) of a bis-adduct, mp > 400 °C. IR ν_{max} (KBr) 1602, 1569, 1487, 695 cm^{-1}; UV λ_{max} ($CHCl_3$) 252 nm (ϵ 92 000), 312 (36 000); ^1H NMR ($CDCl_3$) δ 6.62−6.82, 6.9−7.82, and 7.9−8.02 (34 H, m, methine and aromatic). Anal. Calcd for $C_{100}H_{34}N_2$: C, 95.02; H, 2.71; N, 2.21. Found: C, 95.80. H, 2.51; N, 1.93. Mol wt calcd for $C_{100}H_{35}N_2$ (MH^+) 1264; found, 1264 (FAB). Further characterization of this bis-adduct was not done, and it was not used in the present studies.

Synthesis of the Fullerene−Aniline Dyad (2). A mixture of C_{60} (90 mg, 0.12 mmol), the aldehyde **7** (32 mg, 0.12 mmol), and *N*-methylglycine (11 mg, 0.12 mmol) in toluene (90 mL) was stirred under reflux for 10 h. The reaction was cooled, and removal of the solvent under reduced pressure gave a solid residue, which was chromatographed over silica gel (100−200 mesh). Elution with petroleum ether gave 30 mg (33%) of the unchanged C_{60}. Further elution with a mixture (2:3) of toluene and petroleum ether gave 48 mg (58%) of the fullerene−aniline adduct, **2**, mp > 400 °C. UV λ_{max} ($CHCl_3$) 256 nm (ϵ 115 000), 306 (35 700); IR ν_{max} (KBr) 2932, 2861, 1739, 1600, 1507, 1463, 1427, 1249, 1172, 1035, 825, and 744 cm^{-1}; ^1H NMR ($CDCl_3$) δ 2.85 (3 H, s, NCH_3), 3.0 (3 H, s, NCH_3), 3.6−3.8 (2 H, t, NCH_2) 3.95−4.25 (3 H, m, OCH_2 and CH pyrrolidine ring), 4.8 (1 H, s, CH), 4.95 (1 H, d, CH pyrrolidine ring), and 6.5−7.8 (9H, m, aromatic); ^{13}C NMR ($CDCl_3$), 29.71, 39.16, 39.97, 51.92, 65.15, 68.96, 70.98, 83.13, 112.04, 116.46, 125.29, 128.2, 129.03, 129.14, 129.26, 130.49, 135.74, 135.78, 136.53, 136.77, 139.59, 139.90, 140.11, 140.15, 141.53, 141.67, 141.83, 141.95, 141.99, 142.03, 142.07, 142.12, 142.24, 142.54, 142.67, 142.97, 143.13, 144.38, 144.61, 144.69, 145.14, 145.22, 145.27, 145.33, 145.47, 145.53, 145.77, 146.09, 146.124, 146.20, 146.26, 146.30, 146.33, 146.51, 146.78, 147.29, 148.84, 153.58, 153.62, 154.09, 156.35, 158.70; exact mol wt calcd for $C_{78}H_{22}N_2O$ ($M^{+\bullet}$) 1002.1732l; found, 1002.1725 (FAB high-resolution mass spectrometry).

Preparation of *N*-Methyl-(2-bromoethyl)aniline (6). To an ice cold solution of *N*-methyl-*N*−(2-hydroxyethyl)aniline (**5**) (2.25 g, 15 mmol) in dichloromethane (20 mL) was added PBr_3 (4.05 g, 15 mmol), dropwise over a period of 1 h. The reaction mixture was further stirred at room temperature for an additional period of 3 h. The solvent was removed, and the crude product was chromatographed on silica gel (100−200 mesh) using a mixture (1:10) of ethyl acetate and petroleum ether to give 1.9 g (60%) of **6**. IR ν_{max} (neat) 2929, 1605, 1510, 1373, 1351, 1278, 1214, 1175, 1097, 1035, and 996 cm^{-1}; ^1H NMR ($CDCl_3$), δ 2.95 (3 H, s, NCH_3) 3.2−3.6 (2 H, t, NCH_2), 3.6−3.9 (2 H, t, CH_2), and 6.6−7.5 (5 H, m, aromatic); ^{13}C NMR ($CDCl_3$) δ 146.45, 127.74, 115.42, 110.41, 52.83, 36.90, and 26.87; exact mol wt calcd for $C_9H_{12}NBr$ ($M^{+\bullet}$) 213.0153; found, 213.0142 (FAB high-resolution mass spectrometry).

Preparation of *N*-Methyl-*N*-{(*p*-formylphenoxy)-2-ethyl}-aniline (7). A suspension of the bromide, **6** (0.27 g, 1 mmol), *p*-hydroxybenzaldehyde (0.24 g, 2 mmol), and potassium carbonate (0.28, 2 mmol) was refluxed in acetone (15 mL) for 12 h. The reaction mixture was cooled, filtered, and concentrated under reduced pressure. The residue was chromatographed on silica gel (100−200 mesh) using a mixture (1:10) of ethyl acetate and petroleum ether to give 0.2 g (80%) of **7**. IR ν_{max} (neat) 2934, 2759, 1696, 1602, 1476, 1262, 1161, 1028, and 798 cm^{-1}; ^1H NMR ($CDCl_3$) δ 2.95 (3 H, s, NCH_3), 3.6−3.8 (2 H, t, NCH_2), 4.0−4.3 (2 H, t, OCH_2), 6.4−7.9 (9H, m, aromatic), and 9.8 (1 H, s, CHO); ^{13}C NMR ($CDCl_3$) δ 190.37, 163.67, 148.69, 131.90, 130.17, 129.30, 116.45, 114.74, 112.24, 96.15, 65.69, 51.79, and 39.17; exact mol wt calcd for $C_{16}H_{17}NO_2$ ($M^{+\bullet}$) 255.1259; found, 255.1266 (FAB high-resolution mass spectrometry).

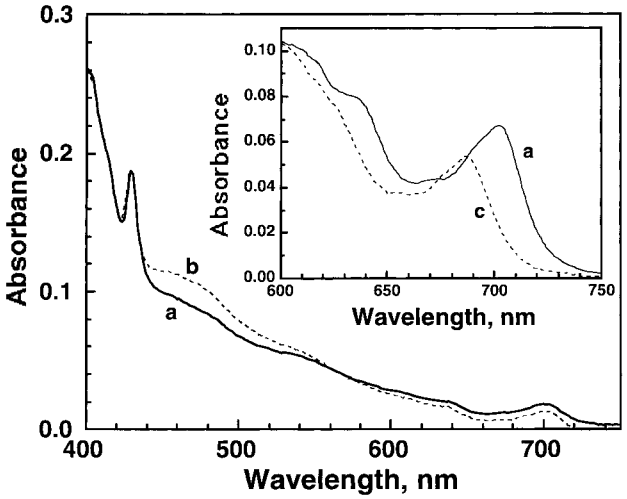

Figure 1. Absorption spectra of dyad **2** (trace a) and model system **1** (trace b), in dichloromethane. Inset shows the changes in the long-wavelength absorption band of dyad **2** in dichloromethane on addition of TFA. The concentrations of TFA were (a) 0 mM and (c) 25 mM.

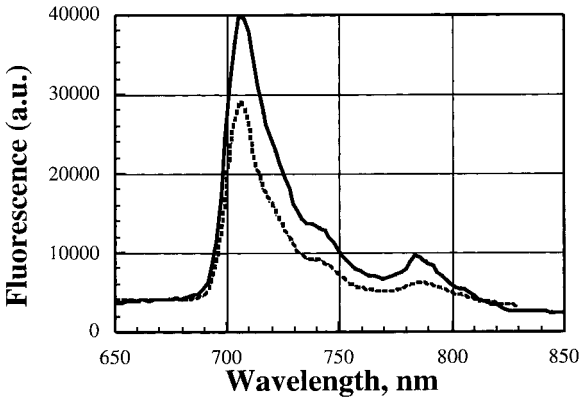

Figure 2. Fluorescence emission spectrum of (a) (—) **1** and (b) (- - -) **2** in methylcyclohexane at 77 K. (The excitation wavelength was at 400 nm.)

Picosecond Laser Flash Photolysis. Picosecond laser flash photolysis experiments were performed with 355-nm laser pulses from a mode-locked, Q-switched Quantel YG-501 DP Nd:YAG laser system (output 1.5 mJ/pulse, pulse width ~18 ps).[30] The white continuum picosecond probe pulse was generated by passing the fundamental output through a D_2O/H_2O mixture. The output was fed to a spectrograph (HR-320, ISDA Instruments, Inc.) with fiber optic cables and was analyzed with a dual diode array detector (Princeton Instruments, Inc.), interfaced with an IBM-AT computer. Time zero in these experiments corresponds to the end of the excitation pulse. All the lifetimes and rate constants reported in this study are at room temperature (297 K) and have an experimental error of ±10%. The deaerated dye solution was continuously flowed through the sample cell during the measurements.

Nanosecond Laser Flash Photolysis. Nanosecond laser flash photolysis experiments were performed with a Laser Photonics PRA/model UV-24 nitrogen laser system (337 nm, 2-ns pulse width, 2−4 mJ/pulse) with front face excitation geometry. A typical experiment consisted of a series of 2−3 replicate shots per single measurement. The average signal was processed with an LSI-11 microprocessor interfaced with a VAX computer. Details of the experimental setup can be found elsewhere.[31]

Pulse Radiolysis. Pulse radiolysis experiments were performed by utilizing 50-ns pulses of 8-MeV electrons from a model TB-8/16-1S Electron Linear Accelerator. Dosimetry was based on the oxidation of SCN^- to $(SCN)_2^{\bullet -}$, which in N_2O-saturated aqueous solutions takes place with $G \sim 6$ (G denotes the number of species per 100 eV, or the approximate micromolar concentration per 10 J of absorbed energy). The radical concentration generated per pulse amounts to $(1-3) \times 10^{-6}$ M for all the systems investigated in this study.

Results and Discussion

Absorption Spectra. The absorption spectra of **1** and **2** recorded in dichloromethane at room temperature are shown in Figure 1. Both show similar absorption properties in the UV region with strong molar absorptivity at 211, 257, 310, and 430 nm. The close resemblance of the absorption pattern of **1** and **2**, with absorption maxima at 701, 690, 680, 667, 655, and 636 nm, with those of various other [6−6] closed fullerene derivatives is indicative of the partial perturbation of the fullerene core. This can be rationalized in view of the fact that monofunctionalization of the fullerene core impacts the electronic structure and leads to a change of the I_h-symmetry of pristine C_{60}, which converts into an effective C_{2v} symmetry.

Absorption spectra of both the compounds in the visible region are significantly red-shifted and distinctly different from that of pristine C_{60}. To investigate the possibility of a ground-state charge-transfer formation at longer wavelengths, trifluoroacetic acid (TFA) was added to dichloromethane solutions of **2**. Dyad **2** possesses a long-wavelength absorption band around 702 nm in dichloromethane, and a hypsochromic shift of 14 nm was observed upon addition of 25 mM of TFA (Figure 1, trace c). These changes can be completely reversed by adding 30 mM of pyridine to the above solution. These results indicate the possibility of ground-state electronic interaction between C_{60} and aniline in dyad **2** as the protonation of nitrogen inhibits such a charge-transfer interaction. In the case of **1**, the absorption spectrum remains unaffected even after adding 250 mM of TFA. Similar effects were observed for other *N*-phenylpyrrolidinofullerenes.[22]

Steady-State Fluorescence. The fluorescence emission spectrum of **1** in methylcyclohexane at 77 K exhibits a maximum at 702 nm (Figure 2). Vibronic fine structure was observed at 715, 725 (sh), 741, 754, 783, 806 (sh), and 824 nm. The structural pattern is in good agreement with other monofunctionalized fullerene derivatives and with the mirror-imaged UV−vis absorption features (see above). Since the distribution of levels in the first-excited state, governing the position of the absorption bands, resembles the distribution of levels in the ground state, which is responsible for the position of the fluorescence bands, fluorescence and absorption features should be very similar. The experimental results show a good mirror image, e.g., the absorption band (0 → *0, 701 nm) of the longest wavelength and the corresponding emission band (*0 → 0, 702 nm) of the shortest wavelength. This further supports an unambiguous assignment of the 0 → 0 transition band.

The emission spectrum of **2** in methylcyclohexane (Figure 2), for example, displays a similar *0 → 0 band at 702 nm, followed by some vibronic states emitting at 715, 725 (sh), 741, 754, 783, 806 (sh), and 824 nm. Although the emission pattern is identical with **1** and various monofunctionalized fullerene derivatives, the relative emission yield of derivative **2** is lower compared to a model fullerene compound. Increasing the

TABLE 1: Fluorescence Quantum Yields (Absolute and Relative) of 1 and 2 in Solvents of Varying Polarity at 77 K

	$\phi_F \times 10^4$ (absolute)	
solvents	**1**	**2**
methylcyclohexane	6.0 (100)	4.4 (100)
toluene		4.2 (95)
dichloromethane		3.8 (86)
toluene−acetonitrile (1:1)		1.9 (43)

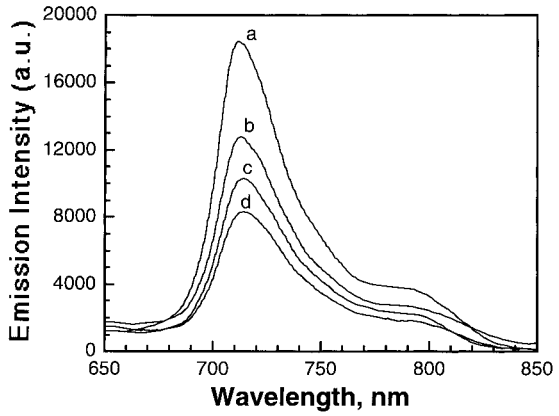

Figure 3. Effect of addition of acetonitrile on the emission spectra of dyad **2** in toluene solution. Acetonitrile v/v (a) 0%, (b) 10%, (c) 30%, (d) 50%. (Corrections for the changes in the absorbance at the excitation wavelength (470 nm) have been made for determining ϕ_f.)

dielectric constant of the solvents resulted in a moderate amplification of this decrease. This observation suggests, in line with the earlier assumption, that intramolecular interaction between the photoexcited fullerene moiety and the aniline group contributes to the overall deactivation process of photoexcited **2**. The emission properties of the *N*-phenyl-substituted pyrrolidinofullerene, **1**, and the dyad, **2**, have been investigated in solvents of a wide range of polarity, and these results are summarized in Table 1. It is interesting to note that **2** exhibits a solvent-dependent fluorescence whereas the emission properties of **1** are independent of the dielectric constant of the solvent.

To investigate the effect of solvent polarity, the emission properties of **2** were studied in toluene−acetonitrile mixtures of varying compositions (Figure 3). A marked decrease in the quantum yield of fluorescence (ϕ_F) was observed upon increasing the polarity of the solvent. The reductive quenching of the singlet excited state of fullerene by aniline moiety is responsible for the decrease in the fluorescence yield in polar solvents. The fluorescence of **2** is restored upon addition of TFA to the above solution. The protonation of nitrogen atom of the aniline group inhibits the electron-transfer process in the donor−acceptor system. Similar effects were earlier observed in fullerene−aniline dyads connected through rigid spacers[20,21] and fullerene−ferrocene dyads.[24] Earlier studies on the photophysical properties of *N*-methylpyrrolidinofullerene have indicated that the pyrrolidine ring nitrogen is not involved in the quenching process.[24] In an earlier study we had found that ϕ_F of **1** ($\sim 6 \times 10^{-4}$) is independent of solvent polarity and that the addition of TFA does not affect its emission properties.[22] However, the aniline group is a good quencher for the singlet excited fullerene. Independent fluorescence-quenching studies carried out with dimethylaniline indicate that singlet excited **1** can be quenched with DMA with a bimolecular rate constant of 3.8×10^{10} M^{-1} s^{-1}.

Steady-State Phosphorescence. External heavy atom effect is known to accelerate the transformation rate from the excited singlet to the excited triplet state. Fullerene related emissions

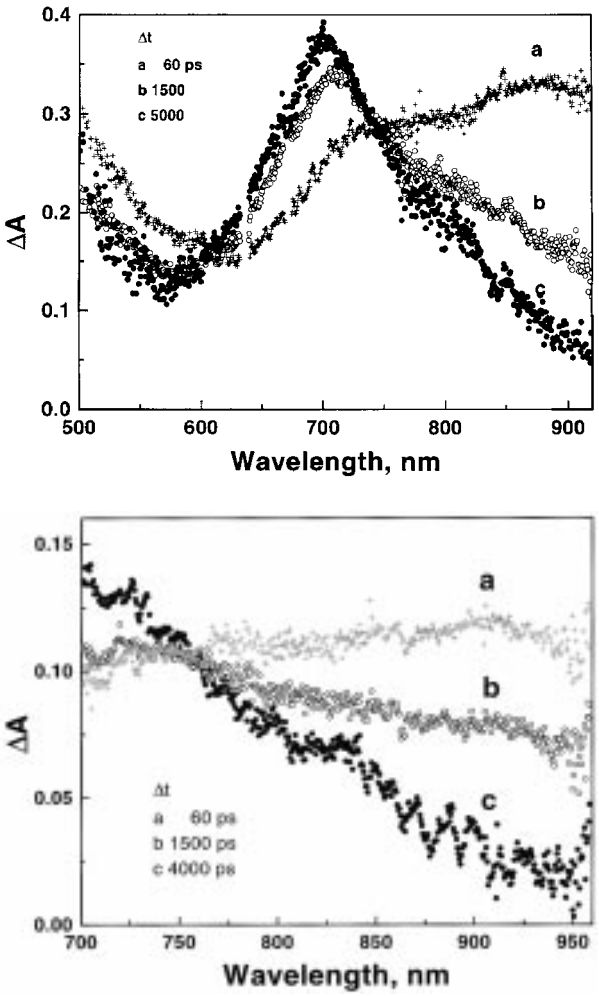

Figure 4. Transient absorption spectra recorded following 355-nm laser pulse (pulse width 18 ps) excitation of toluene solution containing (A, top) **1** at delay times (a) 60, (b) 1500, and (c) 5000 ps and (B, bottom) **2** at delay times (a) 60, (b) 1500, and (c) 4000 ps.

of **1** and **2** were thus completely abolished in solutions containing ethyl iodide (methylcyclohexane, 2-methyltetrahydrofuran, ethyl iodide at 2:1:1 v/v). Instead, a new band appeared at 824 nm that is assigned to the phosphorescence emission. This finding implies a significant red shift of the phosphorescence-related emission relative to pristine C_{60} (796 nm) but is well in line with various monofunctionalized derivatives.

Singlet Excited-State Properties. The excited singlet of pristine C_{60} has an absorption maximum at 920 nm with a lifetime of 1.2 ns, and the triplet excited state has an absorption maximum at 740 nm with a lifetime greater than 100 μs.[33−35] The time-resolved transient absorption spectra recorded following 355-nm laser pulse excitation of the two functionalized fullerenes, **1** and **2**, are shown in Figure 4 A,B. The spectra recorded immediately after 355-nm laser pulse (pulse width 18 ps) excitation show the formation of singlet excited state with a broad absorption maxima in the region of 880 and 890 nm for **1** and **2**, respectively. As the singlet excited state decays, a new absorption band corresponding to the triplet excited state appears with an absorption maximum in the region of 690−700 nm. The intersystem crossing observed in the excited state is quite efficient similar to the one observed for pristine C_{60}. It should be noted that the functionalization of C_{60} has a significant impact on the electronic and spectral properties of the excited state.

The kinetics of excited-state transients was probed by recording absorption−time profiles at different wavelengths. Few representative spectra and decay traces for the dyad **2** are shown in Figure 5A,B. The excited singlet lifetimes of **1** and **2** were obtained from the transient decay recorded at 880 and 890 nm, respectively. The corresponding triplets monitored at 700 nm showed a growth with a rate constant similar to that obtained from the corresponding decay of the singlet excited state. The lifetime of the singlet excited states as monitored from these kinetic traces were 1.25 and 1.05 ns for **1** and **2**, respectively. While the singlet excited lifetime of **1** is not different from that of pristine C_{60}, the singlet excited **2** had a shorter lifetime. The decrease in lifetime observed in these experiments is parallel to the decrease in fluorescence yield observed in higher dielectric media. Presence of a covalently attached aniline functionalizing group, which is a good electron donor, prompts the possibility of an intramolecular quenching with electron transfer.

It should be noted that the photoexcitation of **2** in benzonitrile leads to decreased intersystem-crossing yield. The high dielectric constant of the medium (e.g., benzonitrile relative to toluene, CH_2Cl_2, etc.) is thermodynamically supportive of intermolecular electron transfer. Furthermore, the flexible nature of the linking spacer enables conformational rearrangements of the fullerene and aniline centers. Thus it is conceivable that a combination of these factors increase the thermodynamic driving force for an intramolecular charge-transfer process and, in turn, allow this route to compete with the fast intersystem crossing. The observed shorter lifetime of singlet excited **2** supports this view.

Suggestions have been made in the past that C_{60} undergoes charge-transfer interactions with electron-donating species such as amines in both the ground and excited states.[18,19,32] Similarly charge-transfer complex formation has also been observed in fullerene-donor type dyad moieties. Earlier studies have shown that an excited fullerene-donor complex exhibits a broad absorption in the 700−900-nm region.[19] However, in the present case it was not possible to obtain clean evidence for such an excited charge-transfer complex formation because of the dominance of singlet and triplet absorption in this spectral region. Also, the observation of an isosbestic point between the spectra of singlet and triplet excited states highlights the major contribution from these two species to the transient spectra in Figure 4.

In the case of excited singlet fullerene dyad such as **2**, we expect several possibilities for deactivation including those illustrated in reactions 1−4.

$$C_{60}\text{−X} + h\nu \rightarrow {}^1(C_{60}\text{−X})^* \rightarrow C_{60}\text{−X} + h\nu' \qquad (1)$$

$${}^1(C_{60}\text{−X})^* \rightarrow {}^3(C_{60}\text{−X})^* \qquad (2)$$

$${}^1(C_{60}\text{−X})^* \rightarrow (C_{60}{}^{\bullet-}\cdots X^{\bullet+}) \rightarrow {}^3(C_{60}\text{−X})^* \qquad (3)$$

$${}^1(C_{60}\text{−X})^* \rightarrow (C_{60}{}^{\bullet-}\cdots X^{\bullet+}) \rightarrow (C_{60}\text{−X}) \qquad (4)$$

The intersystem crossing is the major deactivation process in the case of pristine C_{60} and monofunctionalized derivatives. Presence of an electron donor such as the aniline group in **2** adds the possibility of a rapid intramolecular electron-transfer quenching of excited singlet, which competes with intersystem crossing and other deactivation processes. The fluorescence-quenching studies indicated in the previous section strongly support this view. However, the transient absorption studies do not indicate the presence of any charge-separated state. This makes us conclude that either the contribution of intramolecular quenching to the overall decay is small or the charge-separated pair recombines to yield triplet excited state as indicated in reaction 3. The possibility of formation of triplet excited state via recombination of charge-separated pair has been proposed earlier for C_{60}−amine complexes.[33] By comparing the decreased fluorescence yield of **2** in high dielectric media, we estimate the contribution from reactions 3 and 4 to the overall decay to be around 30%. This sets the upper limit for the observed interaction between the two moieties in the excited state of the dyad molecule.

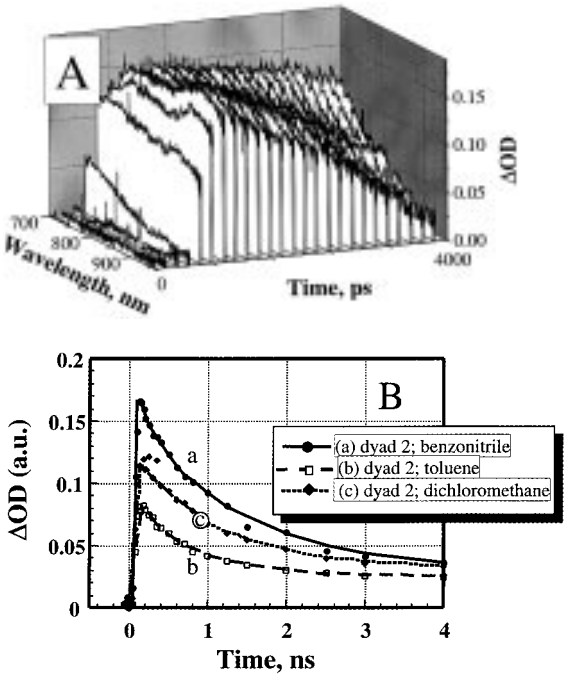

Figure 5. (A) Time-resolved transient absorption spectra showing the decay of singlet and formation of triplet excited states following the 355-nm laser pulse excitation of **2** in toluene. (B) Absorption−time profiles showing the decay of singlet dyad, **2**, in different solvents at monitoring wavelength of 900 nm.

Triplet Excited-State Properties. Nanosecond laser flash photolysis experiments were performed to investigate the triplet excited-state behavior of **1** and **2** in various solvents. The time-resolved transient spectra recorded following 337 (or 355)-nm laser pulse excitation are shown in Figure 6. The spectrum recorded immediately after the laser pulse excitation shows spectral characteristics similar to the long-term spectra in Figure 4. This suggests that the triplet formation be completed within the pulse duration of the excitation pulse. These experiments also enabled us to characterize the absorption bands of triplet excited states in the 350−400-nm region. The spectral characteristics of the triplet excited states are summarized in Table 2.

The time-resolved spectra recorded in Figure 6 did not indicate the formation of any other transients during the deactivation of the triplet excited state. The lifetimes of the triplet excited states of the two title compounds were obtained by fitting the decay traces to first-order kinetics. The lifetimes of the triplet excited states of **1** and **2** were in the range of 7−17 μs. These lifetimes are shorter than the one reported for the triplet excited C_{60}. Although self-quenching processes such as excited-state annihilation and ground-state quenching processes significantly shorten the lifetime of the excited state of

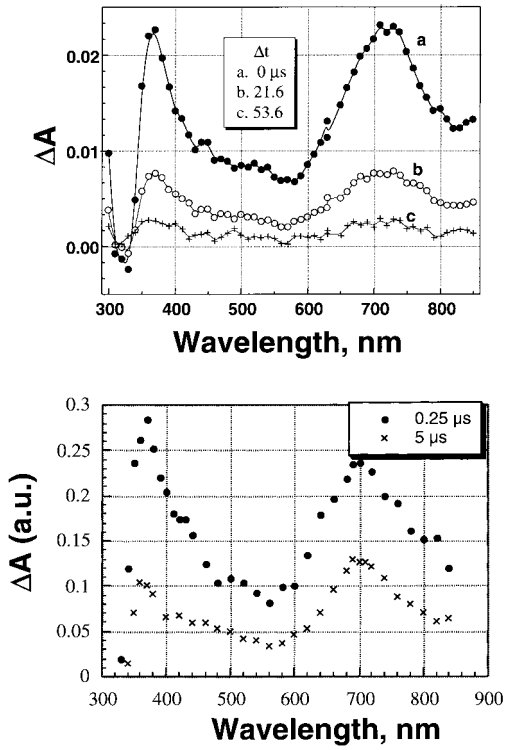

Figure 6. Time-resolved difference absorption spectra recorded following 337-nm laser pulse excitation of (A, top) 1 and (B, bottom) **2** in toluene. The spectra of **1** were recorded at delay times (a) 0, (b) 21.6, and (c) 53.6 μs and those of **2** at 0.25 and 5 μs, respectively, in a nanosecond laser flash photolysis apparatus.

TABLE 2: Excited-State Characteristics

	S_1 (λ_{max})	τ (ps)	T_1 (λ_{max})	τ (μs)
C_{60} (from refs 34, 35, 37)	920	1200	400, 750	>100
1	880	1250 ± 100	690, 370	17 ± 1
2	890	1050 ± 100	700	7 ± 1

fullerenes,[34−36] these processes alone cannot explain the short triplet lifetimes of pyrrolidinofullerenes. A significant destabilization of the fullerene triplet excited state was also evident in corresponding measurements involving dyad **2**. Since the measurements of photoexcited **1** and **2** were conducted under similar experimental conditions, the reduced lifetime, with decay rates typically in the order of 1.25×10^5 s^{-1}, suggests quenching of the photoexcited fullerene moiety by the covalently attached amine group. While the triplet quantum yield of **1** is similar to that of pristine C_{60} ($\Phi = 0.95$),[34,35,37] the triplet quantum yield for **2** was 30% smaller. (We independently measured triplet quantum yield of C_{60}, **1** and **2** by triplet−triplet energy-transfer method using the squaraine dye as an acceptor.[38]) Thus, the lower triplet quantum yield observed for **2** further substantiates the intramolecular quenching of the singlet excited state as a competing process to the intersystem crossing.

In accordance with the accelerated picosecond dynamics, the triplet yield of **2** in benzonitrile was appreciably smaller than in toluene. As discussed in the radiolytic section, π-radical anion's of monofunctionalized fullerenes have a fairly strong absorption around 400 nm, parallel to the coinciding absorption of the triplet excited state (360 nm). The molar absorptivity of the latter is equal or lesser than the dominant ($T_1^* \rightarrow T_n^*$) transition around 700 nm. The differential absorption changes recorded for **2** in benzonitrile indicate, however, a stronger transition around 370−380 nm. Furthermore, the noticeable red-shift can be interpreted as the concomitant generation of

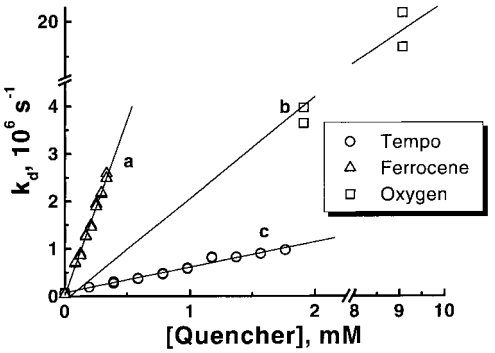

Figure 7. Dependence of pseudo-first-order rate constants for the triplet decay of **2** on the concentration of different quenchers. The triplet decay was monitored at 700 nm.

TABLE 3: Bimolecular Quenching Rate Constants (M^{-1} s^{-1})

	O_2	tempo	ferrocene
C_{60}	1.6×10^9 (ref 42)	3.3×10^9 (ref 39)	3.3×10^9(ref 43)
1	2.14×10^9	6.6×10^8	7.7×10^9
2	2.1×10^9	5.3×10^8	7.4×10^9

two transient species. A complex exponential decay kinetics in the UV prevented, however, a meaningful analysis of the associated processes.

Triplet-State Quenching Reactions. To check the reactivity of the triplet excited states we studied the quenching reactions with three different quenchers, viz., O_2, TEMPO, and ferrocene. The triplet decay at the corresponding absorption maximum was recorded at different quencher concentrations. The bimolecular quenching rate constants were determined from the slope of the plots on basis of the the relationship $k_d = 1/\tau_T + k_q(Q)$, where (Q) is the quencher concentration and τ_T is the lifetime of the triplet excited state in the absence of the quencher. The quenching plots for various quenchers are shown in Figure 7. The rate constants determined from these plots are summarized in Table 3.

The oxygen quenching rate constants for **1** and **2** are very similar ($\sim 2.0 \times 10^9$ M^{-1} s^{-1}). As indicated in previous studies, fullerenes quite efficiently generate singlet oxygen by the energy-transfer method (reaction 5).

$$(^3C_{60})-X^* + O_2 \rightarrow C_{60}-X + {}^1O_2 \qquad (5)$$

Similarly, in the case of ferrocene as a quencher, the rate constants are nearly diffusion-controlled ($(3.6-7.7) \times 10^9$ M^{-1} s^{-1}). The deactivation of the excited triplet state proceeds via electron transfer to ferrocene. However, lack of transient absorbance from long-lived intermediates other than the triplet excited states makes it difficult to elucidate the mechanism of electron-transfer quenching in the present experiments. It should be noted that previous study of the interaction between excited triplet and ferrocene has shown that photoinduced electron transfer can occur in high dielectric media.[24]

The rate constants for the quenching by the stable nitroxyl radical, TEMPO, were very similar for the two compounds, **1** and **2** (6.6×10^8 M^{-1} s^{-1} and 5.3×10^8 M^{-1} s^{-1}, respectively). The excited-state energy transfer to nitroxyl radical is unlikely in the present case since doublet energy for TEMPO (~47 kcal/mol) is significantly higher than the triplet excited states of **1** and **2**, which we expect to be in the range similar to that of $^1C_{60}$* (37.5 kcal/mol). Therefore charge transfer between triplet

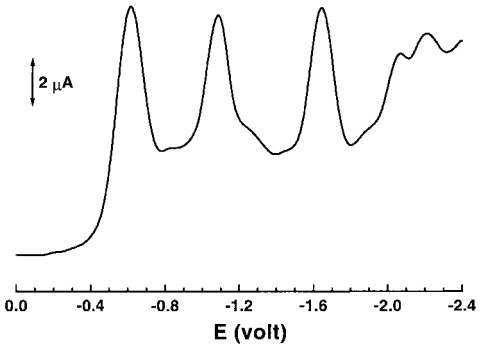

Figure 8. Square-wave voltammogram of **1** in toluene:acetonitrile (3:1 v/v). (Scan rate = 100 mV/s; RE; SCE; WE, glassy carbon; CE, Pt; supporting electrolyte, 0.1 M tetrabutylammonium perchlorate.)

TABLE 4: Reduction Potentials (E_{Red} (mV) vs SCE in Toluene:Acetonitrile (3:1))

	E_1	E_2	E_3	E_4	E_5
C_{60}[a]	−360	−830	−1420	−2010	−2600
1	−648	−1060	−1676	−2100	−2250
2	−585	−1010	−1580	−1980	−2200

[a] In benzene, from ref 44.

excited fullerene and TEMPO seems to be the likely possibility.

$$(^3C_{60})-X^* + TEMPO^\bullet \rightarrow \{(C_{60}^{\bullet-})-X\cdots TEMPO^+\} \rightarrow C_{60}-X + TEMPO^\bullet \quad (6)$$

The lack of observation of radical anions of fullerenes suggests that the back electron transfer of the products is quite efficient and results in regeneration of original reactants. Low dielectric constant of the solvent is likely to favor such a back reaction. Similar observations have also been made in the previous studies involving the quenching of $^3C_{60}$* by various nitroxyl radicals.[39]

Electrochemical Reduction. Fullerenes undergo multiple reductions when subjected to electrochemical and chemical methods. Up to five reversible reductions have been observed for C_{60}. The square-wave voltammetry was employed to obtain the reduction characteristics of the two functionalized fullerenes. An example of successive reduction peaks observed in the square-wave voltammogram of **1** is illustrated in Figure 8. We also recorded cyclic voltammograms to cross-check the assignment of our peak positions and the reversibility of the reduction steps. The reduction potentials of **1** and **2** are compared with that of pristine C_{60} in Table 4. The first reduction occurs in the range of −0.585 to −0.65 V vs SCE, while the second reduction occurred in the region of −1.01 to −1.06 V vs SCE. Other reductions occurred at more negative potentials. It is evident from Table 4 that the functionalization of fullerenes with pyrrolidine moiety has rendered them slightly more difficult to reduce than the pristine C_{60}.

Pulse Radiolytic Formation of π-Radical Anions. Complementary to reductive triplet quenching, radical anions may be produced via radical-induced reduction of the fullerenes. For example, in an irradiated solvent mixture containing 80 vol % toluene, 10 vol % 2-propanol, and 10 vol % acetone, the reducing radical is formed by hydrogen abstraction from 2-propanol.

$$(CH_3)_2CHOH \xrightarrow{\text{radiolysis}} (CH_3)_2{}^\bullet COH \quad (7)$$

The same species derives from acetone upon electron capture and subsequent protonation.

$$(CH_3)_2C{=}O + e_{sol}^- + H^+ \rightarrow (CH_3)_2{}^\bullet COH \quad (8)$$

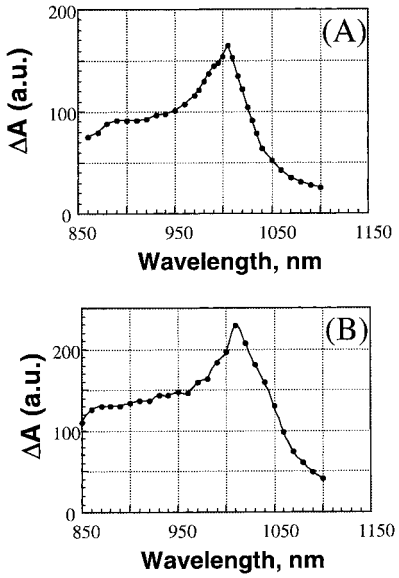

Figure 9. Transient absorption spectrum (near-IR) of (A) **1** and (B) **2** obtained upon pulse radiolysis of 2.0×10^{-5} M of the respective functionalized fullerene derivative in a nitrogen-saturated solvent mixture containing 80 vol % toluene, 10 vol % 2-propanol, and 10 vol % acetone.

This radical is known to react quite rapidly with C_{60}, C_{70}, and C_{84} yielding the respective radical anions, e.g. $C_{60}^{\bullet-}$, $C_{70}^{\bullet-}$, and $C_{84}^{\bullet-}$.[40,41] The same consideration is applied to study one-electron reduction of functionalized fullerenes.

Under these reductive conditions, pulse irradiation of **1** and **2** (2×10^{-5} M) in a deaerated toluene/2-propanol/acetone mixture (8:1:1 v/v) resulted in the formation of distinct and characteristic absorption throughout the UV, visible and near-IR region. The spectra of the reduced form of **1** and **2** are shown in parts A and B of Figure 9, respectively. While the UV part showed sharp bleaching around 320 nm, a range that corresponds to a strong ground-state transition of the fullerene core, the visible region is dominated mainly by maxima around 420 nm. More importantly, the differential absorption spectrum of ($C_{60}^{\bullet-}$) obtained upon pulse radiolysis of **1**, for example, exhibits a distinct maximum at 1005 nm. This characteristic fingerprint for reduced fullerene species is blue-shifted to pristine $C_{60}^{\bullet-}$ (1080 nm), but in close resemblance to the spectral features recorded for the π-radical anion of *N*-methylpyrrolidinofullerene,[24] a structural analogue of **1**. It is a general observation that monofunctionalization leads to a significant blue-shift of the corresponding radical anion bands, and thus, these features are ascribed to the π-radical anion formed in the general reaction.

$$(CH_3)_2{}^\bullet COH + C_{60}-X \rightarrow (CH_3)_2CO + (C_{60}^{\bullet-})-X + H^+ \quad (9)$$

Similarly, the π-radical anion absorption of **2** exhibits a sharp maximum at 1010 nm, nearly identical with **1**.

Conclusions

Pyrrolidinofullerenes exhibit singlet and triplet excited-state properties that differ from those of pristine C_{60}. The time-resolved radiation and photochemical studies have revealed informative details on the influence of functionalized groups on the photophysical properties of functionalized C_{60}. Compared to *N*-phenyl-substituted pyrrolidinofullerene, the *N*-methylaniline−functionalized fullerene dyad shows charge-

transfer interactions in the ground and excited states, which were dependent on the solvent polarity. The triplet quenchers such as O_2, TEMPO, and ferrocene interact with the triplet excited states with bimolecular quenching rate constants of 5.3×10^8 to 7.7×10^9 M^{-1} s^{-1}. The functionalization of fullerenes with pyrrolidine moiety has rendered these pyrrolidinofullerenes slightly more difficult to reduce than the pristine C_{60}.

Acknowledgment. We thank Dr. Di Liu and Mr. Mark R. Flumiani for their assistance in experimentation. P.V.K., D.M.G., and M.V.G. (in part) acknowledge the support from the Office of Basic Energy Science, the U.S. Department of Energy and K.G.T., V.B., and M.V.G. acknowldge the support from the Council of Scientific and Industrial Research, Government of India. One of the authors (M.V.G.) also thanks the Jawaharlal Nehru Centre for Advanced Scientific Research, Bangalore, for financial support. This is contribution No. NDRL 4018 from the Radiation Laboratory and No. RRLT-PRU-86 from RRL, Trivandrum.

References and Notes

(1) Connolly, J. S.; Bolton, J. R. In *Photoinduced Electron Transfer*; Fox, M. A., Channon, M., Eds.; Elsevier: Amsterdam, 1988; p 303.
(2) Kurreck, H.; Huber, M. *Angew. Chem. Res.* **1995**, *34*, 849.
(3) Gust, D.; Moore, T. A.; Moore, A. L. *Acc. Chem. Res* **1993**, *26*, 198.
(4) Arbogast, J. W.; Foote, C. S.; Kao, M. *J. Am. Chem. Soc.* **1992**, *114*, 2277.
(5) Foote, C. S. *Top. Curr. Chem.* **1994**, *169*, 347.
(6) Kamat, P. V.; Asmus, K.-D. *Interface* **1996**, *5*, 22.
(7) Kamat, P. V.; Guldi, D. In *Fullerenes: Chemistry, Physics, and New Directions*; Ruoff, R., Kadish, K., Eds.; Electrochemical Society: Pennington, NJ, 1996; Vol. VIII, p 254.
(8) Sun, Y.-P. In *Molecular and Supramolecular Photochemistry*; Ramamurthy, V., Ed.; Marcel Dekker: New York:, 1997; Vol. 1.
(9) Zhou, F.; Jehoulelt, C.; Bard, A. J. *J. Am. Chem. Soc.* **1992**, *114*, 11004.
(10) Dubois, D. K.; Kadish, K. M.; Flanagan, S.; Haufler, R. E.; Chibante, L. P. E.; Wilsson, L. F. *J. Am. Chem. Soc.* **1992**, *114*, 3978.
(11) Xie, P.; Perez-Cordero, E.; Echegoyen, L. J. *J. Am. Chem. Soc.* **1992**, *114*, 3978.
(12) Wang, Y. *J. Phys. Chem.* **1992**, *96*, 764.
(13) Park, J.; Kim, D.; Suh, Y. D.; Kim, S. K. *J. Phys. Chem.* **1994**, *98*, 12715.
(14) Sun, Y.-P.; Bunker, C. E.; Ma, B. *J. Am. Chem. Soc.* **1994**, *116*, 9692.
(15) Seshadri, R.; Rao, C. N. R.; Pal, H.; Mukherjee, T.; Mittal, J. P. *Chem. Phys. Lett.* **1993**, *205*, 395.
(16) Hirsch, A. *Synthesis* **1995**, 895.
(17) Sun, Y. P.; Ma, B. *Chem. Phys. Lett.* **1995**, *236*, 285.
(18) Sension, R. J.; Szarka, A. Z.; Smith, G. R.; Hochstrasser, R. M. *Chem. Phys. Lett.* **1991**, *185*, 179.
(19) Gevaert, M.; Kamat, P. V. *J. Phys. Chem.* **1992**, *96*, 9883.
(20) Williams, R. M.; Zwier, J. M.; Verhoeven, J. W. *J. Am. Chem. Soc.* **1995**, *117*, 4093.
(21) Williams, R. M.; Koeberg, M.; Lawson, J. M.; An, Y.-Z.; Rubin, Y.; Paddon-Row: M. N.; Verhoeven, J. W. *J. Org. Chem.* **1996**, *61*, 5055.
(22) Kamat, P. V.; Guldi, D. M.; Liu, D.; George Thomas, K.; Biju, V.; S., D.; George, M. V. In *Fullerenes*; Kadish, K., Ruoff, R., Eds.; The Electrochemical Socitey: Pennington, NJ, 1997; Vol. 4, p 122.
(23) Luo, C.; Huang, C.; Gan, L.; Zhou, D.; Xia, W.; Zhuang, Q.; Zhao, Y.; Huang, Y. *J. Phys. Chem.* **1996**, *100*, 16685.
(24) Guldi, D. M.; Maggini, M.; Scorrano, G.; Prato, M. *J. Am. Chem. Soc.* **1997**, *119*, 974.
(25) Kuciavskas, D.; Lin, S.; Seely, G. R.; Moore, A. L.; Moore, T. A.; Gust, D.; Drovetskaya, T.; Reed, C. A.; Boyd, P. D. W. *J. Phys. Chem.* **1996**, *100*, 1592.
(26) Imahori, H.; Hagiwara, K.; Aoki, M.; Akiyama, T.; Taniguchi, S.; Okada, T.; Shirakawa, M.; Sakata, Y. *J. Am. Chem. Soc.* **1996**, *118*, 11771.
(27) Imahori, H.; Cardoso, S.; Tatman, D.; Lin, S.; Noss, L.; Seely, G. R.; Sereno, L.; Chessa de Silber, J.; Moore, T. A.; Morre, A. L.; Gust, D. *Photochem. Photobiol.* **1995**, *62*, 1009.
(28) Catalan, J.; Elguero, J. *J. Am. Chem. Soc.* **1993**, *115*, 9249.
(29) Taylor, T. W. J.; Owen, J. S.; Whitaker, D. *J. Chem. Soc.* **1938**, 206.
(30) Ebbesen, T. W. *Rev. Sci. Instrum.* **1988**, *59*, 1307.
(31) Nagarajan, V.; Fessenden, R. W. *J. Phys. Chem.* **1985**, *89*, 2330.
(32) Sun, Y.-P.; Ma, B.; Lawson, G. E. *Chem. Phys. Lett.* **1995**, *233*, 57.
(33) Ghosh, H. N.; Pal, H.; Sapre, A. V.; Mittal, J. P. *J. Am. Chem. Soc.* **1993**, *115*, 11722.
(34) Ebbesen, T. W.; Tanigaki, K.; Kuroshima, S. *Chem. Phys. Lett.* **1991**, *181*, 501.
(35) Dimitrijevic, N. M.; Kamat, P. V. *J. Phys. Chem.* **1992**, *96*, 4811.
(36) Fraelich, M. R.; Weisman, R. B. *J. Phys. Chem.* **1993**, *97*, 11145.
(37) Biczok, L.; Linschitz, H.; Walter, R. I. *Chem. Phys. Lett.* **1992**, *195*, 339.
(38) Sauve, G.; Kamat, P. V.; Thomas, K. G.; Thomas, J.; Das, S.; George, M. V. *J. Phys. Chem.* **1996**, *100*, 2117.
(39) Samanta, A.; Kamat, P. V. *Chem. Phys. Lett.* **1992**, *199*, 635.
(40) Guldi, D. M.; Hungerbuehler, H.; Janata, E.; Asmus, K. D. *J. Phys. Chem.* **1993**, *97*, 11258.
(41) Kamat, P. V.; Sauve, G.; Guldi, D. M.; Asmus, K.-D. *Res. Chem. Intermed.* **1997**, *23*, 575.
(42) Arbogast, J. W.; Darmanyan, A. P.; Foote, C. S.; Rubin, Y.; Diederich, F. N.; Alvarez, M. M.; Anz, S. J.; Whetten, R. L. *J. Phys. Chem.* **1991**, *95*, 11.
(43) Guldi, D. M.; Maggini, M.; Scorrano, G.; Prato, M. *Res. Chem. Intermed.* **1997**, *23*, 561.
(44) Dubois, D.; Moninot, G.; Kutner, W.; Jones, M. T.; Kadish, K. M. *J. Phys. Chem.* **1992**, *96*, 7137.